

ARMY RESEARCH LABORATORY



**Coulometric Study of Rates of Oxalic Acid Adsorption at a
Polycrystalline Platinum Electrode**

by Sol Gilman

ARL-TR-6165

September 2012

NOTICES

Disclaimers

The findings in this report are not to be construed as an official Department of the Army position unless so designated by other authorized documents.

Citation of manufacturer's or trade names does not constitute an official endorsement or approval of the use thereof.

Destroy this report when it is no longer needed. Do not return it to the originator.

Army Research Laboratory

Adelphi, MD 20783-1197

ARL-TR-6165

September 2012

Coulometric Study of Rates of Oxalic Acid Adsorption at a Polycrystalline Platinum Electrode

Sol Gilman

Sensors and Electron Devices Directorate, ARL

REPORT DOCUMENTATION PAGE

Form Approved
OMB No. 0704-0188

Public reporting burden for this collection of information is estimated to average 1 hour per response, including the time for reviewing instructions, searching existing data sources, gathering and maintaining the data needed, and completing and reviewing the collection information. Send comments regarding this burden estimate or any other aspect of this collection of information, including suggestions for reducing the burden, to Department of Defense, Washington Headquarters Services, Directorate for Information Operations and Reports (0704-0188), 1215 Jefferson Davis Highway, Suite 1204, Arlington, VA 22202-4302. Respondents should be aware that notwithstanding any other provision of law, no person shall be subject to any penalty for failing to comply with a collection of information if it does not display a currently valid OMB control number.

PLEASE DO NOT RETURN YOUR FORM TO THE ABOVE ADDRESS.

1. REPORT DATE (DD-MM-YYYY) September 2012		2. REPORT TYPE Final		3. DATES COVERED (From - To)	
4. TITLE AND SUBTITLE Coulometric Study of Rates of Oxalic Acid Adsorption at a Polycrystalline Platinum Electrode				5a. CONTRACT NUMBER	
				5b. GRANT NUMBER	
				5c. PROGRAM ELEMENT NUMBER	
6. AUTHOR(S) Sol Gilman				5d. PROJECT NUMBER	
				5e. TASK NUMBER	
				5f. WORK UNIT NUMBER	
7. PERFORMING ORGANIZATION NAME(S) AND ADDRESS(ES) U.S. Army Research Laboratory ATTN: RDRL-SED-C 2800 Powder Mill Road Adelphi, MD 20783-1197				8. PERFORMING ORGANIZATION REPORT NUMBER ARL-TR-6165	
9. SPONSORING/MONITORING AGENCY NAME(S) AND ADDRESS(ES)				10. SPONSOR/MONITOR'S ACRONYM(S)	
				11. SPONSOR/MONITOR'S REPORT NUMBER(S)	
12. DISTRIBUTION/AVAILABILITY STATEMENT Approved for public release; distribution unlimited.					
13. SUPPLEMENTARY NOTES					
14. ABSTRACT Quantitative measurement of adsorption/desorption of oxalic acid on a platinum (Pt) electrode from a perchloric acid supporting electrolyte has been accomplished for the first time using a fast potential scan preceded by a sequence of potential steps. From a dilute solution of oxalic acid, adsorption of the anion is so rapid as to be diffusion-controlled over the range of potentials at which the surface is free of adsorbed oxygen; most of the final coverage achieved in less than a half-second. Cathodic desorption of the adsorbed anion occurs in the millisecond range. An isotherm for reversible adsorption applies to the range 0 to 0.9 V versus a reversible hydrogen electrode (RHE), but below 0.3 V, there is conversion to irreversible adsorption that is perceptible after hundreds of seconds. Irreversible adsorption blocks cathodic hydrogen adsorption while reversible adsorption does not. Adsorbed oxalic acid has a negative effect on the anodic oxidation of ethylene glycol and the reduction of molecular oxygen.					
15. SUBJECT TERMS Ion adsorption, oxalic acid adsorption, oxalic acid, ethylene glycol fuel cell, fuel cell					
16. SECURITY CLASSIFICATION OF:			17. LIMITATION OF ABSTRACT UU	18. NUMBER OF PAGES 26	19a. NAME OF RESPONSIBLE PERSON Sol Gilman
a. REPORT Unclassified	b. ABSTRACT Unclassified	c. THIS PAGE Unclassified			19b. TELEPHONE NUMBER (Include area code) (301) 394-0339

Contents

List of Figures	iv
1. Introduction	1
2. Experimental	1
2.1 Supplies and Equipment.....	1
2.2 Electrodes	2
2.3 Procedures	2
2.3.1 Potential Scans	2
3. Results and Discussion	3
3.1 Oxidation of Oxalic Acid	3
3.2 Measurement of the Rates of Rapid Adsorption of Oxalic Acid	3
3.3 Measurement of the Rates of Rapid Desorption of Adsorbed Oxalic Acid	6
3.4 Isotherm for Reversibly Adsorbed Oxalic Acid.....	7
3.5 Slow/Irreversible Adsorption of Oxalic Acid	9
3.6 Effect of Oxalic Acid Adsorption on Anodic Oxidation of Ethylene Glycol	12
3.7 Effect of Oxalic Acid Adsorption on the Cathodic Reduction of Oxygen.....	13
4. Conclusion	15
5. References	16
List of Symbols, Abbreviations, and Acronyms	18
Distribution List	19

List of Figures

Figure 1. CV scan of a 10^{-4} M solution of oxalic acid in 1 N perchloric acid and a sweep speed of 1 mV/s.	3
Figure 2. Representative traces for potential scans after adsorption of oxalic acid from a 10^{-4} M solution in 1 N perchloric acid.....	4
Figure 3. Differential anodic charge corresponding to adsorption of oxalic acid at various potentials from a 10^{-4} M solution of oxalic acid in 1 N perchloric acid at short adsorption times, $v = 1000$ V/s. The straight line corresponds to diffusion control calculated from equation 2, with $n = 2$	6
Figure 4. Differential anodic charge corresponding to desorption at 0.06 V of oxalic acid adsorbed at 0.6 V for 2 s from a 10^{-4} M solution of oxalic acid in 1N perchloric acid.....	7
Figure 5. Potential dependence of coverage with oxalic acid reversibly adsorbed from a 10^{-4} M solution in 1N perchloric acid.....	8
Figure 6. Representative traces of potential scans for oxalic acid irreversibly adsorbed at 0.1 V.....	10
Figure 7. Incremental charge corresponding to oxidation of oxalic acid slowly adsorbed at potentials, U.	11
Figure 8. Differential charges for oxidation, hydrogen blocking of irreversibly adsorbed oxalic acid at 0.1 V from a 10^{-4} M solution.....	12
Figure 9. Traces for anodic scans at 5 mV/s of a 10^{-3} M solution of ethylene glycol in 1N perchloric acid with and without the addition of 10^{-4} M oxalic acid.	13
Figure 10. Traces for cathodic scans at 5 mV/s showing effect of oxalic acid on the cathodic reduction of oxygen.	14

1. Introduction

The adsorption and anodic oxidation of oxalic acid has long been of interest in connection with its use as an analytical (*1*) reagent, and most recently, because it is one of the products of, or rather a final intermediate in, the anodic oxidation of ethylene glycol in an acid fuel cell (*2, 3*). The adsorption of oxalic acid at platinized and platinum (Pt) single crystal electrodes has been studied by a number of electrochemical, isotopic tracer, and spectroscopic techniques (*2–20*). An early study (*3*) of the adsorption on platinized Pt of ^{14}C – labeled oxalic acid from 1N perchloric acid resulted in the conclusion that reversible adsorption occurs between 100 and 600 mV versus a reversible hydrogen electrode (RHE), and that irreversible adsorption occurs at 0.1 V. The speed of the reversible and irreversible adsorptions appeared to be in the range of several minutes for the former and 1–2 h for the latter processes based on the rate of displacement using inactive oxalic acid. Kazarniov et al. (*4*) published a plot of potential dependence of the relative surface coverages with reversible and irreversibly adsorbed oxalic acid species. The reversible fraction was distinguished by its susceptibility to elimination by washing with supporting electrolyte and was judged to be of anionic nature whereas the irreversible fraction was judged to be a –COH species. Using in-situ infrared (IR) spectroscopy and single crystal Pt electrodes, Berna et al. (*4, 5*) concluded that the irreversibly formed, low potential surface species is carbon monoxide (CO), appearing in the bridged configuration at lower coverages and the linear (“atop”) configuration at higher CO coverages. The same authors concluded that the reversibly adsorbed surface species are oxalate or bioxalate ions bonded to the surface via the O and OH groups of the carboxylate groups. Overall, the oxalic acid adsorption studies to date suggest that there is a reversible, and presumably, rapid reversible adsorption of anions at the higher potentials and a relatively slow adsorption irreversible adsorption of CO at low potentials. It was the primary purpose of this study to obtain more quantitative information on the rates of the two types of adsorption

2. Experimental

2.1 Supplies and Equipment

All measurements were made at room temperature (21 °C) in a 1 N solution of perchloric acid with various additions of oxalic acid. The test vessel was fabricated of Pyrex glass containing two platinized Pt counter electrodes isolated from the main compartment by glass frits. The acid solution was prepared using “Millipore” water with a resistivity of 18.2 M-Ω-cm and redistilled perchloric acid (Sigma–Aldrich). The oxalic acid was a Fluka 0.1M reagent. Solutions were de-aerated with reagent grade argon for several hours. Electrochemical measurements were made using a Gamry Reference 3000 potentiostat.

2.2 Electrodes

The working electrode was a commercially pure (CP) grade Pt wire of 0.08 cm diameter. The wire was etched lightly in aqua regia, flame annealed, encased in shrinkable polytetrafluoroethylene (PTFE) tubing to expose a 1-cm length with a geometric area of 0.26 cm^2 and then lightly etched again. The working electrode was periodically immersed in hot chromic acid cleaning solution. Based on cathodic hydrogen deposition as previously described (21) and the assumption of $210 \text{ microcoulombs/cm}^2$ for a smooth Pt surface, the electrode had a hydrogen capacity, sQ_H , of $102 \text{ microcoulombs}$; a roughness factor of 1.9; and a “hydrogen area”, A_H , of 0.49 cm^2 . The value of sQ_H remained constant during several months of experimentation with the electrode.

The two counter electrodes were platinized Pt foils of 1 cm^2 geometric area each. The use of a palladium-hydrogen (Pd/H) electrode as a reference allowed very close placement parallel to the working electrode. It was prepared as described previously (21). The electrode was re-hydrogenated after several days of use and its potential was monitored against a saturated calomel electrode (SCE) in a separate vessel every few hours. Between re-hydrogenations, the electrode was found to maintain a potential of $\sim 0.02 \text{ V}$ within a few millivolts versus the RHE. All potentials applied and reported here were adjusted to that of the RHE.

2.3 Procedures

2.3.1 Potential Scans

Anodic scans were employed to follow the rates of oxalic acid adsorption and desorption. The general approach of using a staircase of pulses to condition the electrode and prepare the surrounding electrolyte for controlled mass transport was described previously (21). The following pretreatment was found to result in an extremely reproducible electrode reference state (e.g., “supporting electrolyte” traces, later shown in figures 2 and 6) that could be maintained for upwards of 1000 s when oxalic acid was not present:

1. 0 V for 1 s to desorb anions (with argon flow)
2. 1.8 V for 2 s to remove oxidizable organics (with argon flow)
3. 1.2 V for 30 s (with argon flow) to maintain electrode passivity while sweeping oxygen away)
4. 1.2 V for 60 s (no argon) to maintain electrode passivity while allowing the electrolyte to become quiescent.
5. Potential step in the range 0.06 to 0.6 V to reduce the electrode surface before scanning.

In the presence of oxalic acid, the surface is free of organic adsorbate at 1.2 V, but unlike the situation for some other organics (e., carbon monoxide [22], ethanol [23]) a Pt electrode is completely passive for oxalic acid oxidation after exposure to high anodic potentials (figure 1).

Some oxidation current continues to flow, necessitating additional potential step(s) to set up the diffusion conditions for the particular experiment, as is discussed in section 3.

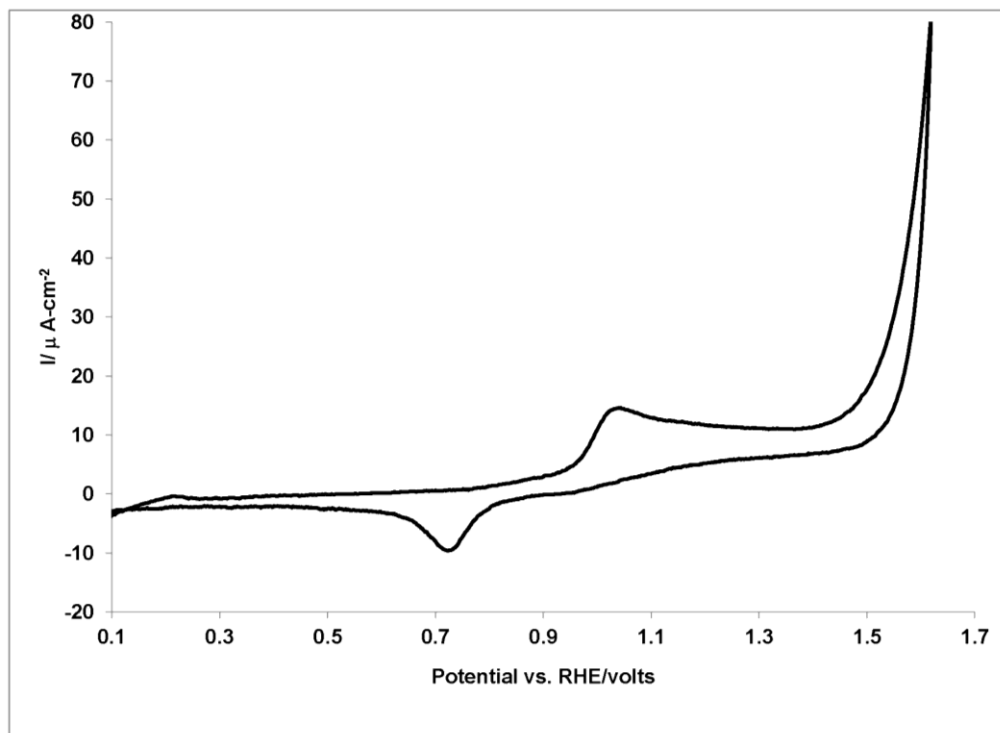


Figure 1. CV scan of a 10^{-4} M solution of oxalic acid in 1 N perchloric acid and a sweep speed of 1 mV/s.

3. Results and Discussion

3.1 Oxidation of Oxalic Acid

The trace of figure 1 was obtained at a linear sweep speed of 1 mV/s after conditioning the electrode as described in section 2.3.1 followed by 1 s at 0.06 V.

The trace shows that no discernible anodic current flows below ~ 0.7 V and that the exposure to high potentials does not fully passivate the electrode against oxidation of oxalic acid as mentioned earlier. Therefore, starting potentials for the adsorption studies in section 3.2 had to be kept below 0.7 V in order to avoid depletion of the adsorbate near the electrode surface. As is discussed in section 3.2, starting potentials had to be further restricted to below 0.1 V to avoid adsorption before the start of the adsorption-rate experiments.

3.2 Measurement of the Rates of Rapid Adsorption of Oxalic Acid

Previous similar studies of the adsorption of the mineral anions, chloride ion (Cl^-) and hydrogen phosphate (HPO_4^-) (24), and acetate ion (21) were accomplished through monitoring of the

quantitative blocking effect of their adsorptions on anodic oxygen adsorption as those ions are not oxidized before the onset of anodic oxygen evolution. The oxidation of adsorbed oxalic acid at higher potentials prevents using the “blocking effect” for following the adsorption processes, but the alternative of measuring oxidative charge passed during an anodic potential scan proved to serve for that purpose as detailed below. The results discussed in this section were obtained for a 0.0001M solution of oxalic acid in 1 N perchloric acid using an anodic scan, sweep speed 1000 V/s, after applying the following sequence of steps:

1. Performing the “cleanup” steps of section 2.3.1, which result in a reproducible surface, but some depletion of oxalic acid at the electrode/electrolyte interface
2. Applying 0.06 V for 20 s with the solution unstirred to establish linear diffusion conditions and enable complete desorption of oxalic acid from the preceding steps. The results discussed in section 3.4 show that the surface is free of irreversibly adsorbed oxalic acid for this period of time and this low concentration of oxalic acid.
3. Applying the adsorption potential U for adsorption time/t

Some representative traces for U = 0.6 V appear in figure 2.

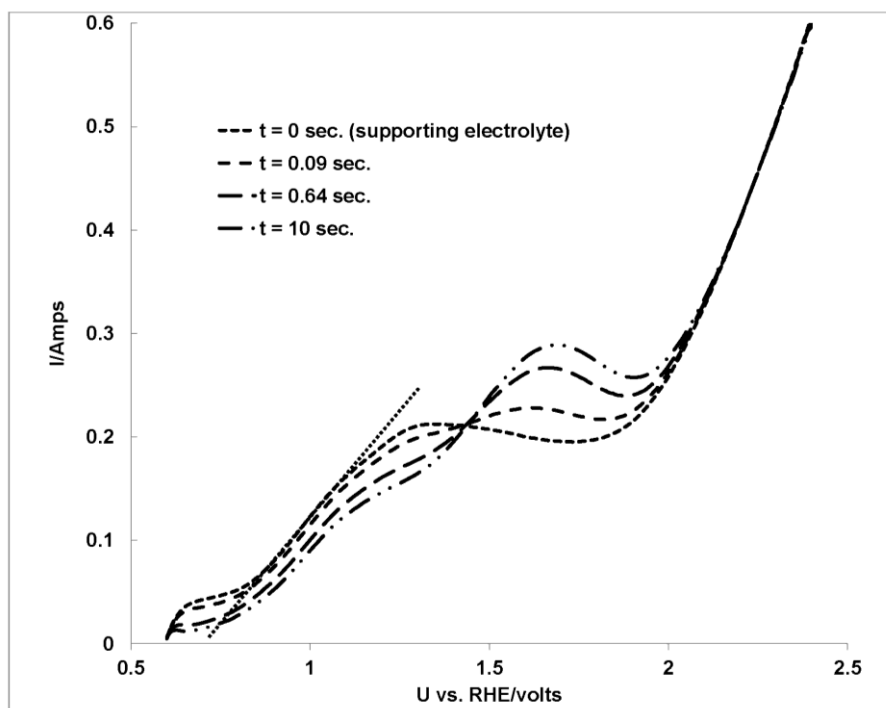


Figure 2. Representative traces for potential scans after adsorption of oxalic acid from a 10^{-4} M solution in 1 N perchloric acid.

Traces for the same value of “t” tend to overlap exactly for the same placement of the electrodes. The charge corresponding to oxidation of the adsorbate was obtained by electronically integrating the closed differential areas (ΔQ) between the solvent trace and the trace for any

value of t , with the traces plotted on the corresponding I /time axes. Values of ΔQ were found to be reproducible to a few tenths of a microcoulomb, the variation attributable mainly to variations in selection of the beginning and ending endpoints for the integration. The assumptions implicit in determining ΔQ were discussed in a previous publication (21). Plots of ΔQ versus $t^{0.5}$ for a range of potentials appear in figure 3. For potentials lower than 0.8 V, the plots are linear, suggesting diffusion-controlled adsorption. Semi-infinite linear diffusion can be expected to apply to the diffusion of oxalic acid to our electrode for small values of t (25):

$$I_d = n\pi^{-1/2}FAD^{1/2}Ct^{-1/2} . \quad (1)$$

Integrating equation 1, the corresponding charge is given by equation 2:

$$Q_d = 2n\pi^{-1/2}FAD^{1/2}Ct^{-1/2} \quad (2)$$

where

n = number of electrons required to oxidize one molecule of adsorbate

F = Faraday constant

A = area = 0.26 cm^2

D = diffusion coefficient of oxalic acid (26) = $1.03 \times 10^{-5} \text{ cm}^2/\text{s}$

The solid straight line in figure 3 was plotted using equation 2, assuming $n = 2$ corresponding to the oxidation of an oxalic acid molecule or ion to carbon dioxide. It can be seen that the data points of figure 3 closely conform to the calculated plot, except for those corresponding to 0.8 V at which potential there is both incipient steady oxidation of both oxalic acid and the platinum surface. The results therefore tend to validate use of the selected anodic scan conditions as a quantitative tool for following adsorption of oxalic acid. Because the adsorptions are so rapid as to be diffusion controlled, kinetic rates may not be determined from the data other than to conclude that the entire process occurs in less than a second at this low concentration.

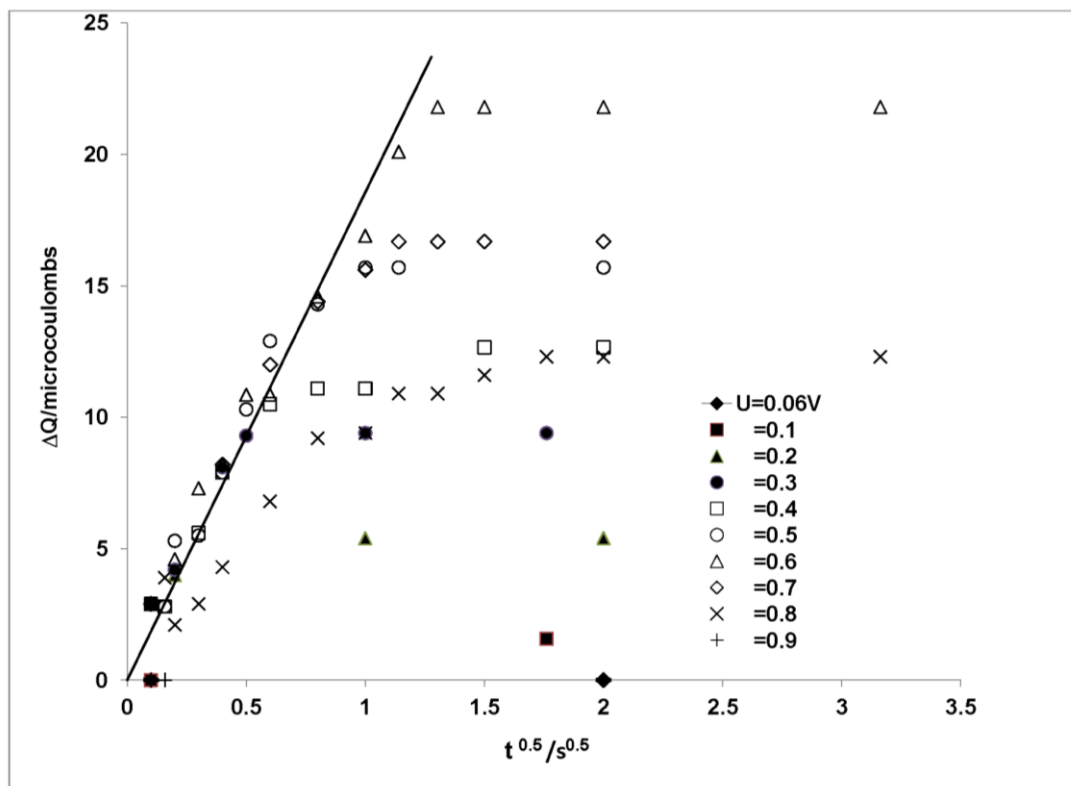


Figure 3. Differential anodic charge corresponding to adsorption of oxalic acid at various potentials from a 10^{-4} M solution of oxalic acid in 1 N perchloric acid at short adsorption times, $v = 1000$ V/s. The straight line corresponds to diffusion control calculated from equation 2, with $n = 2$.

3.3 Measurement of the Rates of Rapid Desorption of Adsorbed Oxalic Acid

For this experiment, oxalic acid was first adsorbed at 0.6 V for 2 s, as described in section 3.2. The potential was then switched to 0.06 V for an interval t_{des} , then back to 0.6 V for 0.2 ms, followed by the measurement scan at 1000 V/s. The resulting values of ΔQ are plotted against the desorption time, t_{des} , in figure 4. Approximately half of the originally adsorbed amount is desorbed within the first 10 ms, followed by slow desorption that continues past 100 s. The possibility that the values of ΔQ in figure 4 include a positive error due to re-adsorption of oxalic acid from the solution must be examined. The pulse/sweep used to measure ΔQ is of ~ 1 ms duration. From figure 3, it can be seen that any diffusion/adsorption from the bulk solution would be negligible in that time period. There is, however, an unknown rate of back-diffusion from the adsorbate expelled during the period t_{des} . A similar experiment with acetic acid desorption involved the similar possibility of re-adsorption and showed complete desorption in less than 1 ms. The desorption of figure 4, occurring much more slowly, is therefore unlikely to include a significant re-adsorption error. Compared to the rate of desorption of acetate ions, the desorption of oxalate ions is ~ 2 orders of magnitude slower. The difference may lie in the

necessity to simultaneously desorb at up to twice as many surface sites for oxalic acid compared with acetic acid.

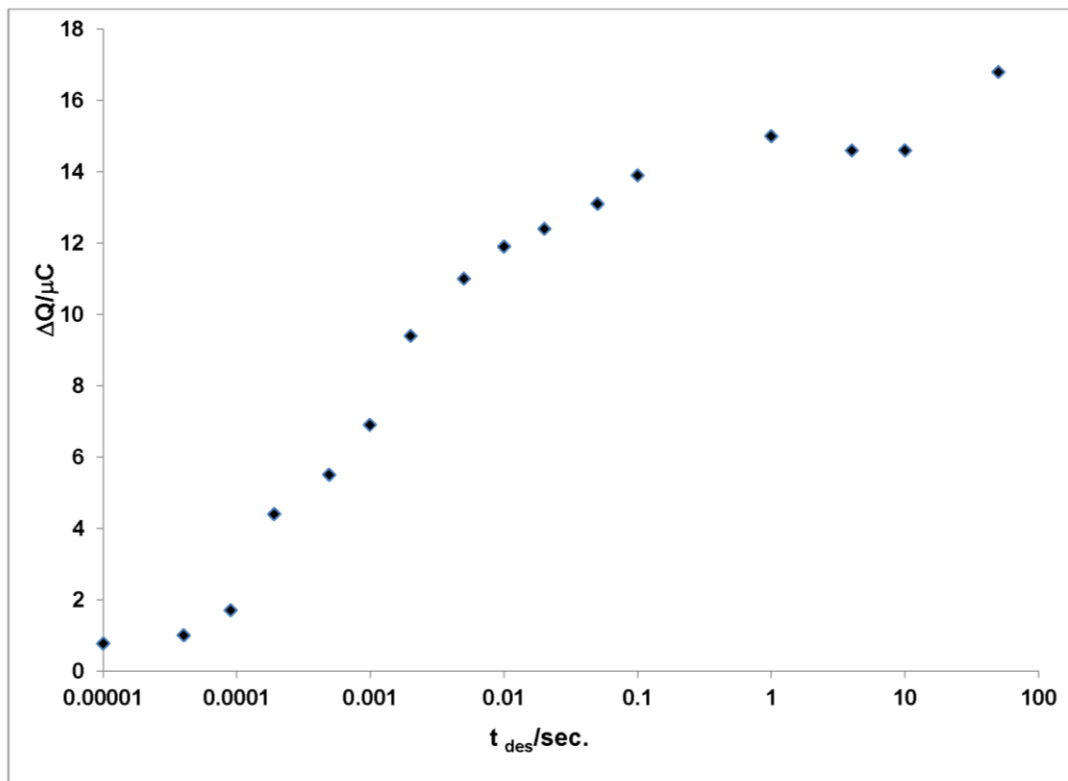


Figure 4. Differential anodic charge corresponding to desorption at 0.06 V of oxalic acid adsorbed at 0.6 V for 2 s from a 10^{-4} M solution of oxalic acid in 1N perchloric acid.

3.4 Isotherm for Reversibly Adsorbed Oxalic Acid

The plateau values of figure 3 correspond to what has been identified by Berna et al. (5) as the reversible adsorption of oxalic acid as oxalate and bioxalate ions. Values of ΔQ measured after 4 s of adsorption were converted to “surface excess” using equation 3:

$$\Gamma = \Delta Q / 2FA_H, \quad (3)$$

where Γ = surface excess

ΔQ = Differential charge

F = Faraday constant

A_H = Hydrogen area (0.49 cm^2)

The dependence of Γ on potential is plotted in figure 5.

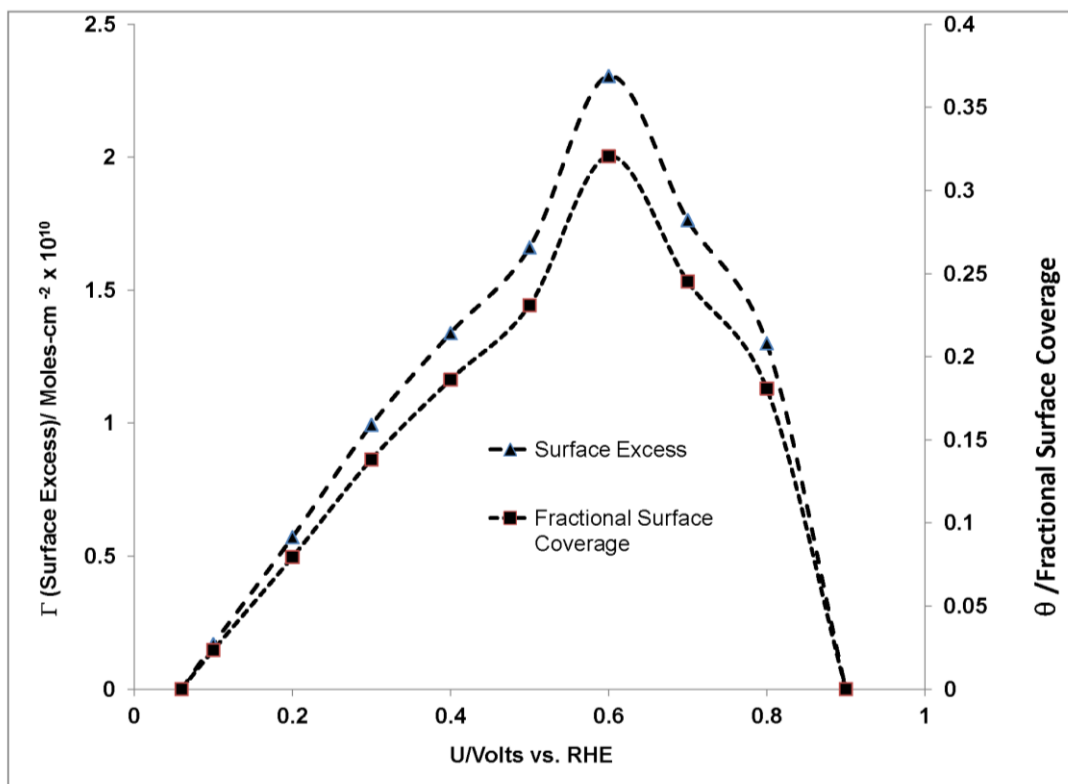


Figure 5. Potential dependence of coverage with oxalic acid reversibly adsorbed from a 10^{-4} M solution in 1N perchloric acid.

A tentative conversion of the ΔQ values to fractional surface coverage of (hydrogen) adsorption sites can be based on the following assumptions:

1. Each carboxylate group is bonded to the surface in a “bridged” mode (i.e., occupies two hydrogen adsorption sites). This assumption is supported by the evidence for two-site adsorption of acetic acid (21).
2. The average number of carboxylate groups/molecule of oxalic acid is ~ 1.5 , corresponding to the conclusion (5) that the adsorbed species is a combination of oxalate and bioxalate ions.

Assumptions 1 and 2 imply that there is an average occupancy of three adsorption sites per molecule of oxalic acid.

Based on assumptions 1 and 2, values of fractional surface coverage were calculated using equation 4 and plotted on figure 5.

$$\theta = 1.5\Delta Q/sQ_H, \quad (4)$$

here sQ_H corresponds to monolayer coverage with hydrogen = 102 microcoulombs (see section 2.2). ΔQ involves a two-electron oxidation (from section 3.2) and is equivalent to two hydrogen

sites. Kazarinov et al. (18), through the use of radiotracers, reported a value of $\theta = 0.3$ at 0.6 V, which is in excellent agreement with the value of 0.32 from figure 5. Their values represent the fraction of total carbon in both ionic and non-ionic form (discussed in section 3.4). The very close agreement is probably fortuitous considering the different methods of measurement and different bases for calculating θ .

Referring to figure 5, the initial approximately linear rise in surface coverage from ~0.06 to 0.6 V is what prompted early investigators to conclude that the adsorption is anionic in nature, as mentioned in section 1. The rather sharp decline to 0 at 0.9 V occurs in a region of potentials in which there is the beginning of both oxidation of the Pt surface and the steady oxidation of oxalic acid to carbon dioxide (see figure 1). Both events likely contribute to the steep decline in surface coverage with oxalate ions.

3.5 Slow/Irreversible Adsorption of Oxalic Acid

It has already been noted (11, 18–20) that at potentials below ~0.4 V versus RHE, there is the slow accumulation of material on a Pt electrode. Unlike the anionic adlayer resulting at higher potentials or after short durations at the lower potentials, the slowly accumulated adlayer cannot be removed by washing the electrode and has been identified (5) as adsorbed CO. The results discussed in this section were obtained using an anodic scan, sweep speed of 1000 V/s, after applying the following sequence of steps:

1. The “cleanup” steps at 0, 1.8, and 1.2 V of section 2.3.1 that results in a reproducible surface
2. Potential U, for adsorption time, t_{ads}

Unlike the situation for studying the rapid adsorptions of section 3.2, a starting potential at 0.06 V (to establish linear diffusion conditions) could not be employed, because that hold-off condition only applies to the low concentration (0.0001M) of oxalic acid used in the experiments discussed in that section. The procedure used in this section as described earlier results in some depletion of oxalic acid at the electrode/electrolyte interface at $t = 0$ s due to incomplete passivation of the surface to oxidation of oxalic acid after the 1.2-V step (see figure 1). However, that can have no significant effect on the adsorption rates reported in this section because these rates are very slow and clearly not diffusion-controlled.

Some representative potential scan traces appear in figure 6.

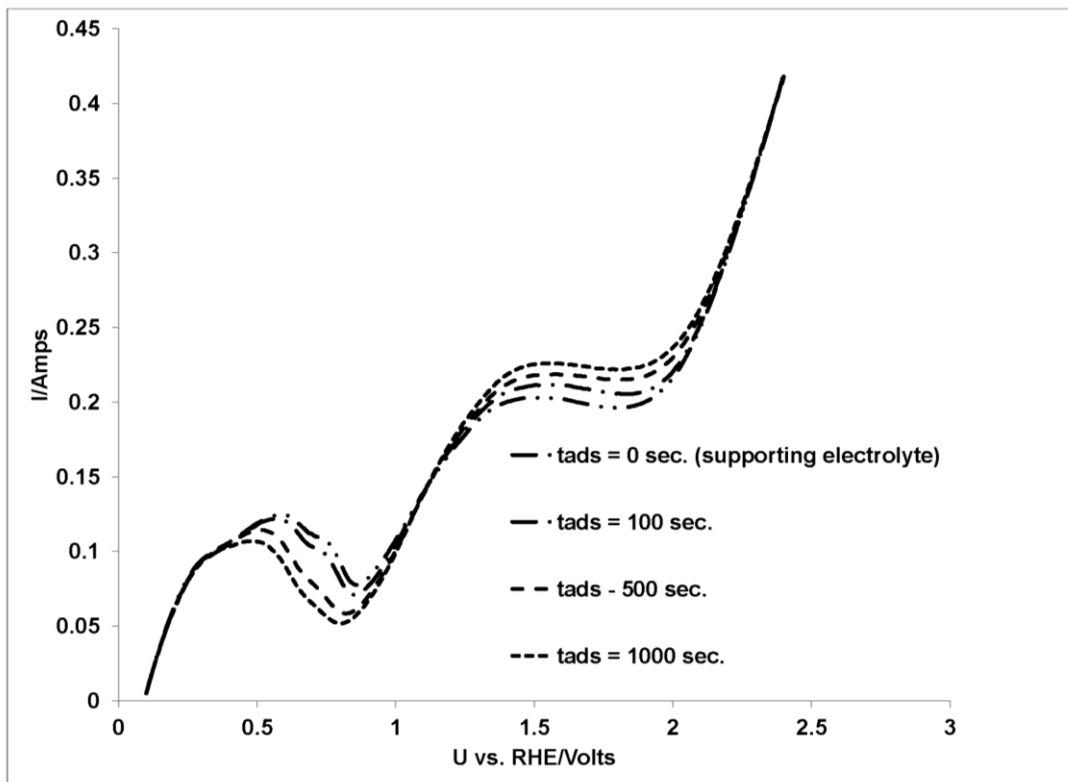


Figure 6. Representative traces of potential scans for oxalic acid irreversibly adsorbed at 0.1 V.

The figure shows the increases in charge at high scan potentials corresponding to oxidation of adsorbed oxalic acid and corresponding decreases in the charge at low scan potentials corresponding to decreases in adsorbed hydrogen. Values of ΔQ_{ox} and ΔQ_H were obtained by integrating the closed areas in the two potential ranges. Values of ΔQ_{ox} for a number of adsorption potentials and oxalic acid concentrations are plotted in figure 7.

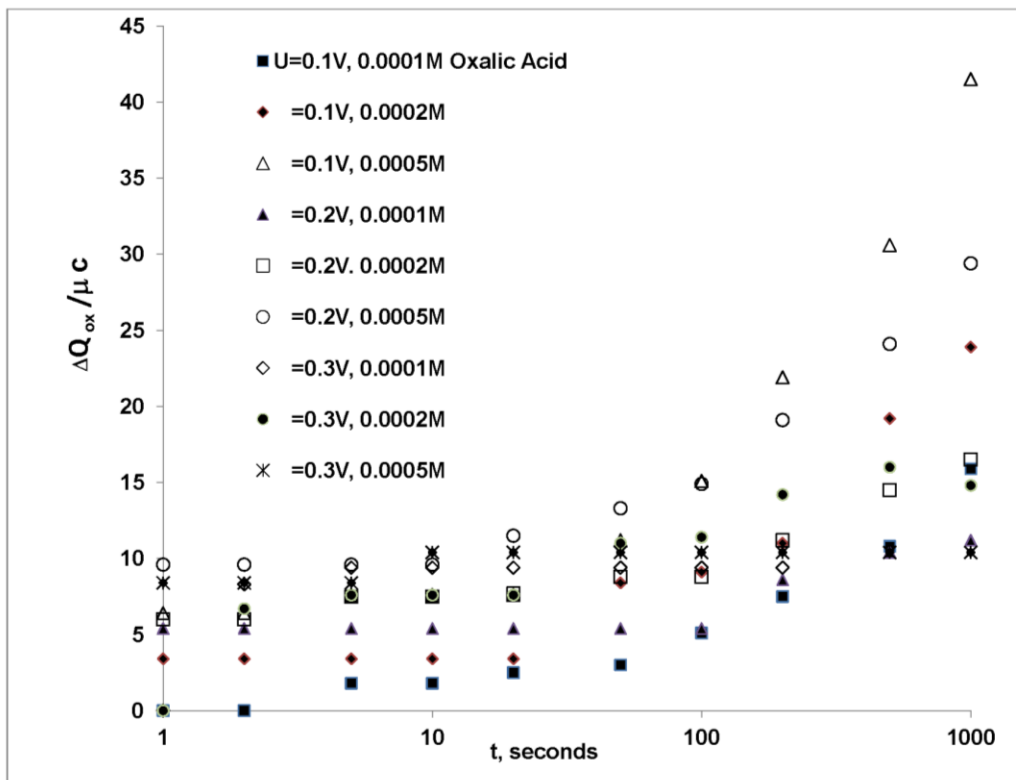


Figure 7. Incremental charge corresponding to oxidation of oxalic acid slowly adsorbed at potentials, U .

From figure 7, it can be seen that there is little change in ΔQ_{ox} during the first 10 s of adsorption for all potentials and concentrations. Significant increases in amounts adsorbed are apparent starting at ~ 20 s, with the largest increase occurring at the lowest potentials and highest concentrations. Increases in ΔQ_{ox} continue past 1000 s but were not followed past this time due to limitations due to electrolyte purity. This contrasts with the plateau values for reversible adsorption that were reached by 1 s at the lowest concentration of oxalic acid.

Values of ΔQ_{ox} and ΔQ_H obtained for adsorption at 0.1 V from 10^{-4} M oxalic acid are plotted in figure 8.

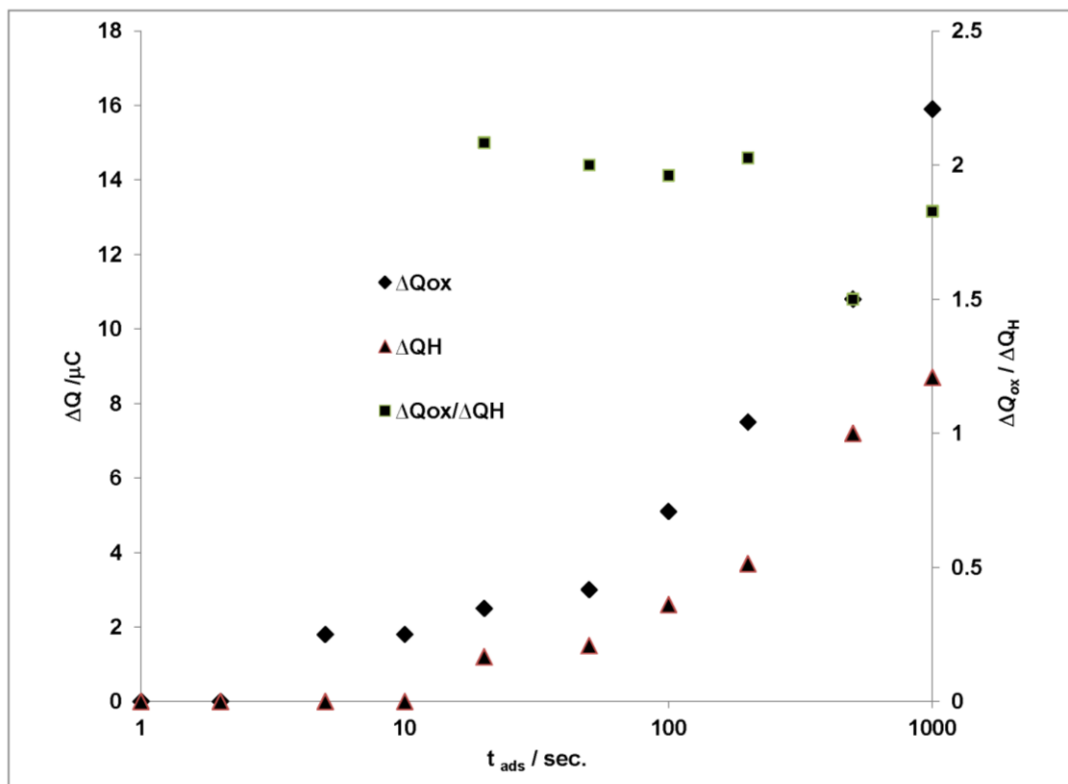


Figure 8. Differential charges for oxidation, hydrogen blocking of irreversibly adsorbed oxalic acid at 0.1 V from a 10^{-4}M solution.

It can be seen from figure 8 that the decrease in charge corresponding to adsorbed hydrogen parallels the increase in charge corresponding to oxidation of adsorbed oxalic acid, and that the ratio of the latter to the former quantity approximates 2. This implies a predominately one-site, i.e., linear, attachment of CO to each hydrogen adsorption site under these conditions.

3.6 Effect of Oxalic Acid Adsorption on Anodic Oxidation of Ethylene Glycol

Oxalic acid is one of the final products of anodic oxidation of ethylene glycol in experimental fuel cells (2, 3). It is therefore of interest to examine the effect that its accumulation may have on the glycol oxidation rate. The traces of figure 9 were obtained by pretreating the electrode as described in section 2.3.1, then holding the electrode at a potential of 0.3 V for 1 s or at 0.1 V for 200 s, followed by a 5 mV/s linear anodic potential scan. Traces 1a and 1b involve a starting potential for which only anion adsorption of oxalic acid occurs, according to section 3.4. Also, at this slow sweep speed, it can be expected that in the absence of ethylene glycol the surface coverage with acetate ion would follow figure 5. In the presence of ethylene glycol, we could expect some displacement of the anion by glycolic species with the balance of the anionic adsorbate acting as a poison to the oxidation of glycol. The traces beginning at 0.4 V in figure 9 surprisingly show no poisoning effect until the potential exceeds ~ 0.5 V, which may imply that the anion adsorption has been reduced below a critical level by adsorbed glycol. Above 0.5 V,

the effect of adsorbed oxalate is quite noticeable, increasing the overvoltage by ~0.1 V and halving the maximum current of the first peak. For the traces following exposure to 0.1 V for 200 s, figure 7 shows that there would initially be a significant buildup of the irreversibly adsorbed species that has been identified as CO. That adsorbate produces a very significant poisoning effect at the earliest scan potentials, as seen in figure 9. Traces 2a and 2b correspond to a starting condition for which the adsorption of oxalic acid results in adsorbed CO, according to the results of section 3.4. No replacement of strongly adsorbed CO by ethylene glycol would be anticipated and the pronounced poisoning effect (trace 2b vs. trace 2a) on ethylene glycol oxidation is evident from the beginning of the potential scan. The peak at 1.0 V corresponds to oxidation of oxalic acid. For an ethylene glycol fuel cell, these results suggest that accumulated oxalic acid product would not have a significant effect on the anodic overvoltage when operating at the lower range of current densities with avoidance of exposing the electrode to hydrogen potentials.

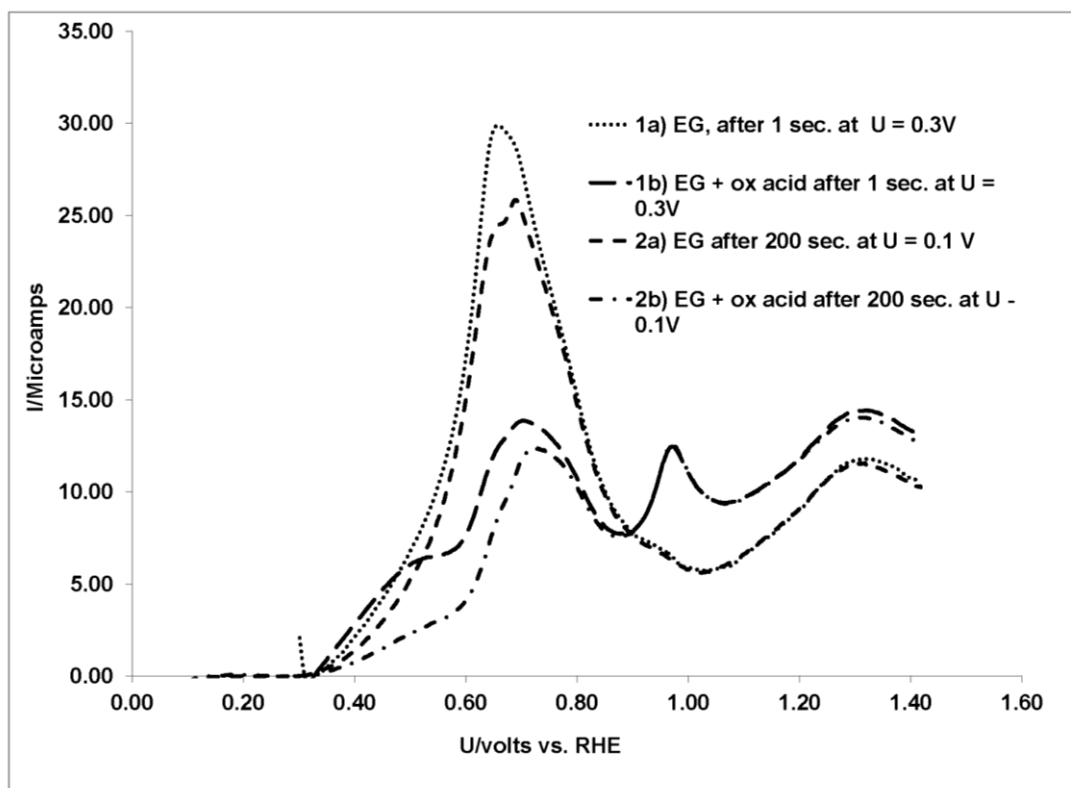


Figure 9. Traces for anodic scans at 5 mV/s of a 10^{-3} M solution of ethylene glycol in 1N perchloric acid with and without the addition of 10^{-4} M oxalic acid.

3.7 Effect of Oxalic Acid Adsorption on the Cathodic Reduction of Oxygen

Oxalic acid produced as a final product of ethylene glycol oxidation may be expected to diffuse to some extent to the air cathode of a fuel cell. In that connection, it is of interest to explore the effect of adsorbed oxalic acid on the oxygen electrode.

The traces of figure 10 were obtained at a sweep speed of 1 mV/s after cleaning and reducing the Pt surface at 0.4 V following steps 1–5 of section 2.3.1. Following step 5, the potential was held at 0.95 V (~open circuit potential for the oxygen electrode) for 30 s. At that point, the solution adjacent to the electrode should be at the same concentration levels as in the bulk. The electrode surface would be expected to be reduced and free of adsorbates other than some atomic oxygen. Trace 3 shows the relatively small anodic current obtained for a solution of 0.0001M oxalic acid in 1 N perchloric acid. That current would be expected to have subtracted only slightly from the cathodic currents of traces 2 and 3. The shift to higher overvoltages (tens of millivolts) represented by trace 3 versus 2 can be ascribed to the adsorption of oxalic acid as the anion, roughly following the equilibrium coverages of figure 5.

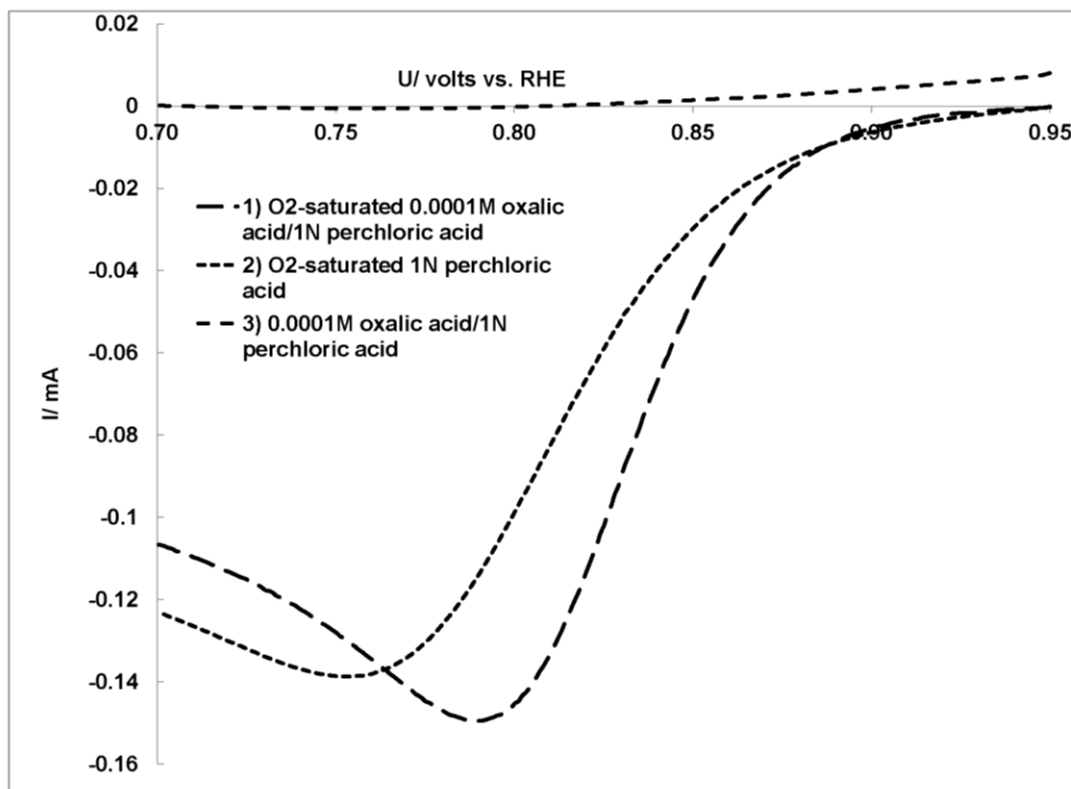


Figure 10. Traces for cathodic scans at 5 mV/s showing effect of oxalic acid on the cathodic reduction of oxygen.

4. Conclusion

With the appropriate “staircase” of potential steps, the adsorption/desorption of oxalic acid may be tracked quantitatively with high resolution using a fast potential scan. The adsorption of oxalic acid in anionic form is rapid and diffusion-controlled over the full range of adsorption potentials. In a 10^{-4} M solution of oxalic acid in 1 N perchloric acid, this translates into the achievement of equilibrium coverage in 1 s or less. Equilibrium coverage with oxalate/bioxalate occurs in the potential range 0.1 to 0.9 V, peaking at 0.6 V. The drop to 0 coverage at 0.9 V coincides with both the onset of significant steady oxidation of oxalic acid and oxidation of the Pt surface. Oxalate/bioxalate ions adsorbed at 0.6 V from a 10^{-4} M oxalic acid solution are almost completely desorbed in 0.1 s. By comparison, desorption of adsorbed acetate ions can occur in a millisecond. The difference may be due to the necessity for simultaneous desorption at up to twice the adsorption sites/molecule. Irreversible adsorption to adsorbed CO occurs at hydrogen adsorption potentials. At 0.1 V, and oxalic acid concentrations in the range 10^{-4} to 5×10^{-4} M oxalic acid, significant adsorption begins after ~ 10 s and adsorption continues past 1000 s. Oxalic acid is one of the products of anodic oxidation of ethylene glycol in experimental fuel cells. Oxalic acid increases the overvoltage both for the oxidation of ethylene glycol and the reduction of oxygen, with a possible net effect on the operating voltage of an ethylene glycol fuel cell in the tens of millivolts range.

5. References

1. Sljukic, B.; Baron, R.; Compton, R. G. *Electroanalysis* **2007**, *19*, 918–922.
2. Livshits, V.; Philosoph, M.; Peled, E. *Journal of Power Sources* **2008**, *178*, 687.
3. de Lima, R. B.; Paganin, V.; Iwasita, T.; Vielstich, W. *Electrochimica Acta* **2003**, *49*, 85–91.
4. Berná, A.; Rodes, A.; Feliu, J. M. *J. Electroanal. Chem* **2004**, *563*, 49–62.
5. Berná, A.; Rodes, A.; Feliu, J. M. *Electrochimica Acta* **2004**, *49*, 1257–1269.
6. Sargisyan, S. A.; Vasil'ev, Yu. B. *Elektrokhimya* **1981**, *17*, 1495–1500.
7. Ferro, S.; Martí'nez-Huitle, C. A.; De Battisti, A. *J Appl Electrochem* **2010**, *40*, 1779–1787.
8. Horanyi, G.; Solt, J. *J. Electroanal. Chem* **1971**, *31*, 95–102.
9. Horanyi, G.; Vertes, G.; Hegedus, D. *Acta Chimica Acad. Scientiarum Hungaricae, Tomus* **1973**, *79*, 301–322.
10. Horanyi, G.; Vertes, G. *Electroanal. Chem. and Interfacial Electrochem.* **1973**, *43*, 225–231.
11. Horanyi, G.; Hegedus, D.; Rizmayer, E. M. *J. Electroanal. Chem* **1972**, *40*, 393–398.
12. Horanyi, G.; Rizmayer, E. M. *J. Electroanal. Chem* **1978**, *93*, 183–194.
13. Inzelt, G.; Szetey, E. *Acta Chimica Acad. Scientiarum Hungaricae, Tomus* **1981**, *107*, 269–284.
14. Li, S.; van der Est, A.; Bunce, N. J. *Electrochimica Acta* **2009**, *54*, 3589–3593.
15. Chollier-Brym, M. J.; Eprom, F.; Lamy-Pitara, E.; Barbier, J. *J. Electroanal. Chem* **1999**, *474*, 147–154.
16. Orts, J. M.; Feliu, J. M.; Aldaz, A.; Clavilier, J.; Rodes, A. *J. Electroanal. Chem.* **1990**, *281*, 199–219.
17. Smirnova, S. W.; Petrii, O. A.; Grzejdzia, A. *J. Electroanal. Chem.* **1988**, *251*, 73–87.
18. Kazarinov, V. E.; Vassiliev, Y. B.; Andreev, V. N. *J. Electroanal. Chem.* **1983**, *147*, 247–261.
19. Vassiliev, Y. B.; Sarghisyan, A. *Electrochimica Acta* **1986**, *31*, 645–655.
20. Wang, H.; Jusys, Z.; Behm, R. J. *Electrochimica Acta* **2009**, *54*, 6484–6498.
21. Gilman, S. *Electrochimica Acta* **2012**, *65*, 141–148.

22. Gilman, S. *J. Phys. Chem* **1963**, *67*, 78–84.
23. Gilman, S. *J. Power Sources* **2012**, *197*, 65–71.
24. Gilman, S. *J. Phys. Chem* **1964**, *68*, 2098–2010.
25. *New Instrumental Methods in Electrochemistry*; Interscience Publishers, Inc., New York, NY, 1959, p. 62.
26. Slukic, B.; Baron, R.; Compton, R. G. *Electroanalysis* **2007**, *19*, 918–922.

List of Symbols, Abbreviations, and Acronyms

Cl ⁻	chloride ion
CO	carbon monoxide
CP	commercially pure
HPO ₄ ⁻	hydrogen phosphate
IR	infrared
Pd/H	palladium-hydrogen
Pt	platinum
PTFE	polytetrafluoroethylene
RHE	reversible hydrogen electrode
SCE	saturated calomel electrode

1 DEFENSE TECHNICAL
(PDF INFORMATION CTR
only) DTIC OCA
8725 JOHN J KINGMAN RD
STE 0944
FORT BELVOIR VA 22060-6218

1 DIRECTOR
US ARMY RESEARCH LAB
IMAL HRA
2800 POWDER MILL RD
ADELPHI MD 20783-1197

1 DIRECTOR
US ARMY RESEARCH LAB
RDRL CIO LL
2800 POWDER MILL RD
ADELPHI MD 20783-1197

1 DIRECTOR
US ARY RESEARCH LAB
RDRL CIO LT
2800 POWDER MILL RD
ADELPHI MD 20783-1197

6 HCS US ARMY RSRCH LAB
RDRL SED E J SHAFFER
RDRL SED C
C LUNDGREN
D CHU
R JIANG
W BEHL
J READ
ADELPHI MD 20783-1197

1 HC CERDEC HDQ
ATTN EDWARD PLICHTA
5100 MAGAZINE ROAD
ABERDEEN PROVING GROUND, MD 21005

INTENTIONALLY LEFT BLANK.